An MD study of methane diffusion in zeolites of structure type LTA

S. Fritzsche[a], R. Haberlandt[a], J. Kärger[a], H. Pfeifer[a] and M. Waldherr-Teschner[b]

[a]Universität Leipzig, Fakultät für Physik und Geowissenschaften
Linnéstraße 5, D-04103 Leipzig, Germany

[b]Silicon Graphics AG
Erlensträsschen 65, CH-4125 Riehen, Switzerland

Diffusion of methane in zeolites of structure type LTA is simulated by Molecular Dynamics (MD) calculations. Small variations of the Lennard-Jones parameters (determining the window size) and the nature of the considered exchangable cations are found to be of decisive importance for the observed dependences, leading to self-diffusivities which may both increase and decrease with increasing concentration. The different patterns of molecular propagation and their microdynamic origin are visualized by video demonstrations. Taking into account the gradient of the chemical potential as a driving force for the diffusion process the transport-diffusivity is found to increase with increasing concentration.

1. INTRODUCTION

The investigation of diffusion processes in zeolites is of great importance [1,2]. Covering the gap between the stimulating forces for molecular random walk and macroscopic diffusion phenomena, MD simulations have proven to be of decisive relevance for the theoretical foundation of experimentally determined diffusivities and for their correlation with the rate determining mechanisms. Systematic studies of this type [3] are of special relevance for current attempts to explain remaining differences between the results of different diffusion experiments (in particular of equilibrium and nonequilibrium techniques) on the basis of differences in the microdynamic situation.

In our simulations we have considered methane in zeolite NaCaA (fig.1) and in its cation-free analogue both of the structure type LTA [4]. It is in particular the simple structure of the latter system which permits simulations of the motion of guest molecules through the zeolite lattice over a large range of parameters (observation time, temperature, concentration, Lennard-Jones radii and potential minima) with a high statistical accuracy.

Typical features of the trajectories are visualized by video demonstrations using a Silicon Graphics workstation.
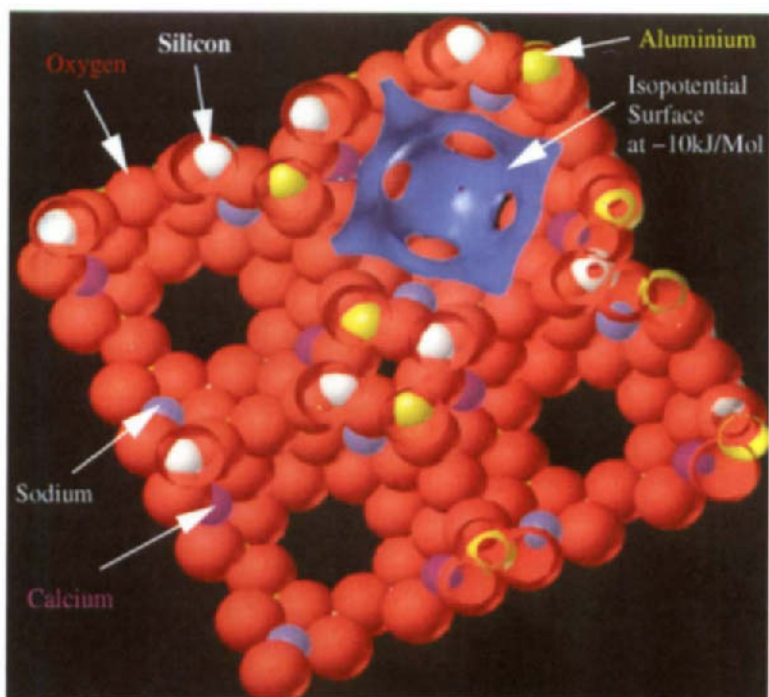
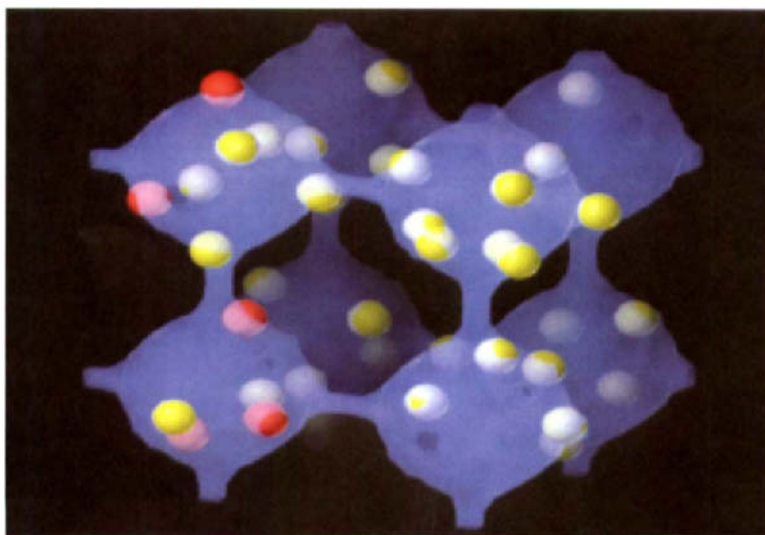Figure 1. Cut through the zeolite NaCaA .

Figure 2. CH$_4$ molecules in a zeolite of type LTA symbolized by isopotential surfaces.

2. SIMULATIONS

The simulations were carried out by means of the velocity Verlet algorithm [4,5] with timesteps of 5 and 10 fs, respectively. Depending on the loading, the basic MD box contains 8 up to 343 large cavities with values for the total occupation number between 256 and 448. These large values yield a high statistical accuracy (error < 3%) for the cation-free zeolite of type LTA. The mean error of the diffusion data for NaCaA is much larger due to the smaller diffusion coefficients, demanding much longer computation times.

Starting with an arbitrary, but relatively homogeneous, configuration, the system evolution is simulated over an equilibration period of 20 000 time steps for the cation-free zeolite of type LTA to get a realistic fluctuation state. Then the evaluation is carried out during at least 150 000 time steps for the cation-free zeolite of type LTA and up to 2 500 000 for NaCaA.

As an example figure 2 shows a snapshot of the molecular distribution in the intracrystalline pore system of structure type LTA as symbolized by its isopotential surface with -9kJ/mol at 300K. The loading corresponds to a sorbate concentration of $I = 5$ molecules per cavity. At the beginning of the simulation run the "red" molecules were located in the lower left cavity.

Because of the nearly spherical shape of the methane molecule the Lennard-Jones (LJ) (12,6) potential $U(r)$

$$U(r) = 4\epsilon \left\{ \left(\frac{\sigma}{r}\right)^{12} - \left(\frac{\sigma}{r}\right)^{6} \right\},$$ (1)

with ϵ as the potential minimum and σ defined by $U(\sigma) = 0$, is well suited to describe the methane-methane interaction [6]. The potential energy of a single methane molecule at different positions along the window axis up to the cavity center is given for two potential models (A,B) in figures 3,4 for the cation-free LTA and NaCaA, respectively. Performing
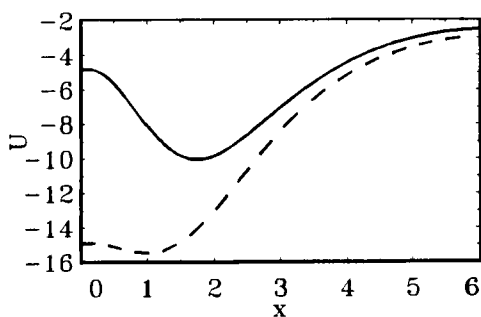

Figure 3. The potential energy (in kJ/mol) (- - - model A , — model B) of a single methane molecule along the window axis (in Å) for the cation-free LTA.
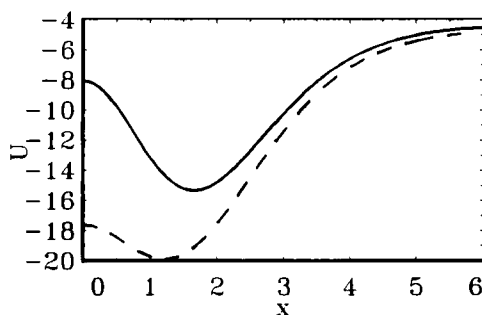
Figure 4. The potential energy (in kJ/mol) (- - - model A , — model B) of a single methane molecule along the window axis (in Å) for NaCaA.

the calculations we use two different potentials (A,B). They are based on the following sets of potential parameters. Model A: CH_4-CH_4: $\sigma = 3.817\text{\AA}$, $\epsilon = 1.232$ kJ/mol; CH_4-O: $\sigma = 3.14\text{\AA}$, $\epsilon = 1.5$ kJ/mol; CH_4-Si: $\sigma = 2.14\text{\AA}$, $\epsilon = 0.29$ kJ/mol [7]; Model B: as model A, but with CH_4-O changed to $\sigma = 3.46\text{\AA}$, $\epsilon = 0.81$ kJ/mol. These values are used in [8] and with a small modification also in [9], while in [10,11] and [12] interaction parameters identical or similar to those of model A are used.

The structure of NaCaA is given in figure 1. It shows four "large cavities". Each of them is surrounded by 8 cubooctrahedra. The large cavity may therefore be visualized by a cube, whose corners are represented by the cubooctahedra. The large cavities are connected with their neighbours by 6 windows, each of them in one of the sides of the imagined cube. The absence of cations in the case of the cation-free zeolite of type LTA and the vanishing dipole moment of the methane molecule allow us to take into account short range intermolecular forces only, while for NaCaA due to the exchangeable cations polarization energies must be considered additionally.

To evaluate the diffusion coefficient we use Einstein's equation

$$< (\vec{r} - \vec{r}_0)^2 > = 6Dt, \tag{2}$$

with the mean square displacement (MSQD) $< (\vec{r} - \vec{r}_0)^2 >$ of the moving particles. This expression can be easily derived from the solution of the diffusion equation. It is equivalent to the expression

$$D = \frac{1}{3} \int_0^\infty < \vec{r}(t)\vec{r}(0) > dt \tag{3}$$

based on the velocity autocorrelation function $< \vec{r}(t)\vec{r}(0) >$ [2,6]. The applicability of eq.(2) - which is by no means trivial for finite diffusion paths - was shown in [11] by comparing the D values resulting from different moments n $(n = 1, 2, 3, 4)$

$$< |\vec{r} - \vec{r}_0|^n > = \int |\vec{r} - \vec{r}_0|^n P(\vec{r}, \vec{r}_0, t) d\vec{r} \tag{4}$$

of the distribution

$$P(\vec{r}, \vec{r}_0, t) = (4\pi Dt)^{-3/2} exp \left\{ \frac{-(\vec{r} - \vec{r}_0)^2}{4Dt} \right\}. \tag{5}$$

The coincidence of the thus calculated diffusion coefficients D is necessary and sufficient for the validity of the diffusion equation, so that in this case eq.(2) can be used to determine D.

As an example, figure 5 shows the diffusion coefficients for methane in cation-free zeolite of type LTA following from different moments, calculated by the MD runs for a mean occupation number $I = 3$ at 300K in dependence on the observation time t. It can be seen that these values approach each other for $|t - t_0| \sim 40 - 60$ ps. The molecular distribution is thus found to follow eq.(5), so that eq.(2) is an appropriate starting point to calculate D. On the contrary, for NaCaA much longer times are neccesary (see fig.6), ranging from $10 - 30\,000$ps in dependence on the loading.

In general, instead of eq.(2) the expression

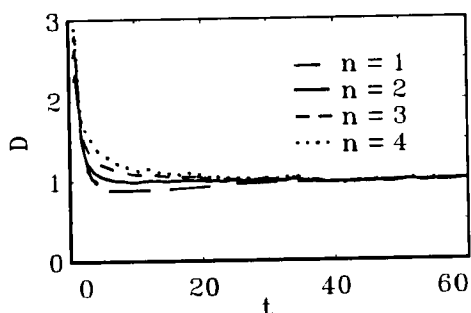$$D = \frac{1}{6} \frac{d}{dt} < (\vec{r} - \vec{r}_0)^2 >, \tag{6}$$

Figure 5. Values for the diffusion coefficient D (in 10^{-8}m^2/s) of CH$_4$ in cation-free LTA (parameter set A) at 300K for a mean occupation number of $I = 3$ molecules per cavity determined from the moments $n = 1, \cdots, 4$ in dependence on the observation time t (in ps).
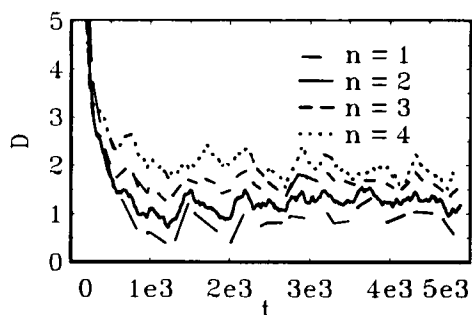
Figure 6. Values for the diffusion coefficient D (in 10^{-11}m^2/s) of CH$_4$ in zeolite NaCaA (parameter set B) at 173K for a mean occupation number of $I = 5$ molecules per cavity determined from the moments $n = 1, \cdots, 4$ in dependence on the observation time t (in ps).

and analogous formulas for the other moments, are used because the slope which defines D in eq.(6) reaches the final value more rapidly than the D value following from eq.(2).

3. RESULTS AND DISCUSSION

The calculated diffusion coefficients are found to be in satisfactory agreement with an Arrhenius law of the form

$$D(I,T) = D_0(I)exp\left\{ -\frac{E_0(I)}{k_B T} \right\}, \tag{7}$$

which is shown in figure 7 for a cation-free zeolite of type LTA.

In the cation-free zeolite a reduction of the window diameter (by an enhancement of the Lennard-Jones parameter σ_{CH_4-O}) leads to a dramatic decrease in the absolute values of the diffusivities and, simultaneously, to a reversed concentration dependence, i.e. to diffusivities increasing with increasing concentration.

Figure 8 shows values for the diffusion coefficient in dependence on the potential parameter σ_{CH_4-O} for two different loadings at temperature $T = 300$K (model A). Comparing the curves for low ($I = 1$) and high loading ($I = 6$) it can be seen that for large windows (about $\sigma \leq 3.25$Å) (model A) the diffusion coefficient decreases with increasing loading while it increases with increasing loading for smaller windows (about $\sigma \geq 3.25$Å) (model B). This is shown in figure 8, by comparing the diffusivities obtained for two different loadings with the parameter σ of the CH$_4$-O interaction varied within the range used in literature [7–12].

This behaviour corresponds to the measured concentration dependence of the self-diffusion coefficient of methane in NaCaA zeolites [13,14] ($4 \cdot 10^{-10}$m^2/s and $8 \cdot 10^{-10}$m^2/s
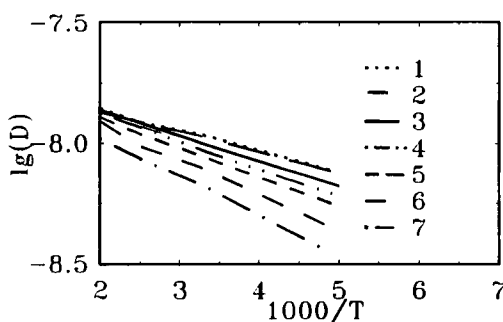
Figure 7. The Arrhenius law for the diffusion coefficient. Logarithm of D (D in m^2/s) versus $1000/T$ (in 1/K) for cation-free LTA zeolite (Model A).
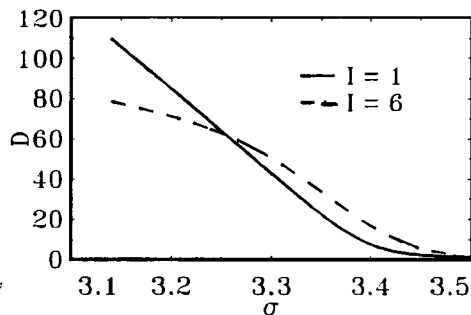
Figure 8. The diffusion coefficient D (in 10^{-10}m^2/s) for cation-free LTA at 300K as a function of σ_{CH_4-O} (in Å) for $I = 1$ and $I = 6$ methane molecules per cavity.

for 1 and 3 molecules per cavity at 173K. However, due to the presence of electric charges, the polarization interaction will lead to a quite different mechanism of the diffusion in NaCaA [15] so that conclusions from the cation-free zeolite of type LTA to this zeolite are by no means straightforward. More detailed calculations for zeolite NaCaA are the object of a forthcoming paper [16].

As a first result, the inclusion of the adsorbate-cation interaction has been found to lead to dramatically reduced diffusivities, which increase with increasing sorbate concentration. These tendencies are in satisfactory agreement with the results of PFG NMR measurements [17].

The influence of the window diameters, of the cation content and of the sorbate concentration on molecular diffusion is distinctly reflected in the trajectories. A quantity characterizing molecular propagation along a given trajectory is the time τ between succeeding passages through the windows between adjacent cavities. Figure 9 shows the probability density w of the thus defined "residence times" within the individual cavities for three different sorbate concentrations (model A). The first maximum at ~ 0.3 ps corresponds to times which are too short to allow a passage through the cavity to one of the five other windows. Therefore, this maximum must be attributed to trajectories, which are reversed immediately after the molecule has passed the window. It is interesting to note that the intensity of this first maximum increases with inreasing sorbate concentration. It may be concluded, therefore, that the reversal in the trajectory is mainly caused by the influence of the other adsorbate molecules. This conclusion is convincingly supported by video demonstrations.

The second maximum corresponds to those passages, which effectively contribute to molecular propagation.

Only very recently MD simulations have been applied to investigate molecular transportation under nonequilibrium conditions [3]. Figure 10 provides a comparison of the various diffusivities of the system under study (cation-free LTA with an analytical model

potential at 300K) obtained under equilibrium and nonequilibrium conditions [18]. It is interesting to note that the self-diffusion as obtained by calculating the mean square displacement under equilibrium conditions (MSQD □) and under nonequilibrium conditions in the plane perpendicular to the concentration gradient (NEMSQDXY ◇) completely coincide. As intuitevely anticipated, molecular propagation under the influence of a concentration gradient is thus found to remain unaffected in the plane (XY) perpendicular to the concentration gradient. By contrast, molecular propagation in the direction of the concentration gradient (Z) is substantially affected, leading to the transport diffusities D_T evaluated by Fick's law (NEMD ▽) presented in figure 10. In agreement with the conventional way of correlating transport- and self-diffusities on the basis of the Darken relation [2]

$$D_T \approx \frac{D}{k_B T} \frac{d\mu}{d\ln c} \qquad (8)$$

the thus defined transport diffusivities (Wid △) agree in the tendency with the NEMD data, where the chemical potential μ has been evaluated by the method of Widom [19]. In both cases, the transport diffusivities are found to increase with increasing concentration c. Such a behaviour is generally observed in uptake measurements with light paraffins in zeolite LTA [2].
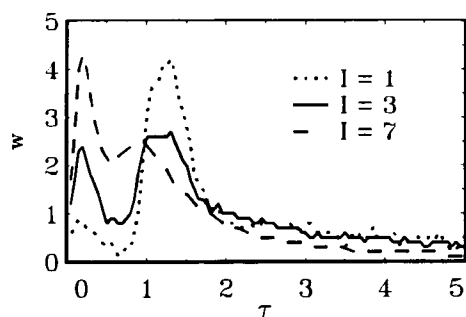

Figure 9. Distribution function w for the residence times τ (in ps) of methane molecules in a given cavity for different loadings $I = 1, 3, 7$ at 300K (model A).
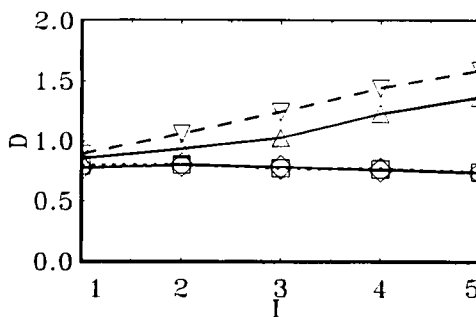
Figure 10. Comparison of equilibrium and nonequilibrium values of D (in 10^{-8}m^2/s) in dependence of the loading I (MSQD □, NEMSQDXY ◇, NEMD ▽, Wid △) .

REFERENCES

1. General Discussion , J. Chem. Soc. Faraday Trans. 87(1991)1797.
2. J. Kärger, D.M. Ruthven: Diffusion in zeolites and other microporous solids, Wiley, New York 1992.
3. E.J. Maginn, A.T. Bell, D.N. Theodorou, J. Phys. Chem 97(1993)4173.
4. S. Fritzsche, R. Haberlandt, J. Kärger, H. Pfeifer, K. Heinzinger, Chem. Phys. 174 (1993)229.
5. M.P. Allen, D.J. Tildesley: Computer simulation of liquids, Clarendon Press, Oxford 1989.
6. M. Schoen, C. Hoheisel, Mol.Phys. 58(1986)699.
7. A.G. Bezus, A.V. Kiselev, A.A. Lopatkin, P.Q. Du, J. Chem. Soc. Faraday Trans. II 74(1978)367.
8. D.M. Ruthven, R.I. Derrah, J. Chem. Soc. Faraday Trans. I 68(1972)2332.
9. P. Demontis, E.S. Fois, G.B. Suffritti, S. Quartieri, J. Phys. Chem. 94(1990)4329.
10. S. Fritzsche, R. Haberlandt, J. Kärger, H. Pfeifer, M. Wolfsberg, Chem. Phys. Lett. 171(1990)109.
11. S. Fritzsche, R. Haberlandt, J. Kärger, H. Pfeifer, K. Heinzinger, Chem. Phys. Lett. 198(1992)283.
12. S.J. Goodbody, K. Watanabe, D. MacGowan, J.P.R.B. Walton, N. Quirke, J. Chem. Faraday Trans. 87(1991)1951.
13. J. Kärger, H. Pfeifer, J. Chem. Soc. Faraday Trans. 87(1991)1989.
14. W. Heink, J. Kärger, H. Pfeifer, P. Salverda, K.P. Datema, A. Nowak, J. Chem. Soc. Faraday Trans. 88(1992)515.
15. G. Schrimpf, M. Schlenkrich, J. Brickmann, P. Bopp, J. Phys. Chem. 96(1992)7404.
16. S. Fritzsche, R. Haberlandt, J. Kärger, H. Pfeifer, M. Wolfsberg, H. Heinzinger, (in preparation).
17. W. Heink, J. Kärger, S. Ernst, J. Weitkamp, Zeolites 14(1994), in press.
18. S. Fritzsche, R. Haberlandt, J. Kärger, Z.phys.Chem., (in preparation).
19. B. Widom, J. Chem. Phys. 39(1963)2808.